

## Noise-Induced Hopf-Bifurcation-Type Sequence and Transition to Chaos in the Lorenz Equations

J. B. Gao,<sup>1</sup> Wen-wen Tung,<sup>2</sup> and Nageswara Rao<sup>3</sup>

<sup>1</sup>*Department of Electrical and Computer Engineering, EB 559, University of Florida, Gainesville, Florida 32611*

<sup>2</sup>*Department of Atmospheric Sciences, University of California, Los Angeles, California 90095*

<sup>3</sup>*Mailstop 6355, P.O. Box 2008, Oak Ridge National Laboratory, Oak Ridge, Tennessee 37831-6355*  
(Received 19 July 2002; published 27 November 2002)

We study the effects of noise on the Lorenz equations in the parameter regime admitting two stable fixed point solutions and a strange attractor. We show that noise annihilates the two stable fixed point attractors and evicts a Hopf-bifurcation-like sequence and transition to chaos. The noise-induced oscillatory motions have very well defined period and amplitude, and this phenomenon is similar to stochastic resonance, but without a weak periodic forcing. When the noise level exceeds certain threshold value but is not too strong, the noise-induced signals enable an objective computation of the largest positive Lyapunov exponent, which characterize the signals to be truly chaotic.

DOI: 10.1103/PhysRevLett.89.254101

PACS numbers: 05.45.-a, 47.27.Sd

Noise is ubiquitous in nature and man-made systems, such as nonlinear solid state devices, physiological systems, and fluid flows. In nonlinear dynamical systems, noise can induce a number of interesting phenomena, including stochastic resonance [1] (for a recent review, see [2]), noise-induced instability [3,4], noise-induced order [5], and noise-induced chaos [6–11].

To gain new insights into the effects of noise on a dynamical system, in this Letter we study the Lorenz equations with parameters admitting multiple stable attractors. It has been found that multistability is common for a variety of nonlinear systems including electronic circuits [12], lasers [13], geophysical models [14], mechanical systems [15], and biological systems [16] such as neurons [17], human proprioceptive system [18], and visual perception [19,20]. Earlier works on the effects of noise on dynamical systems with multiple stable attractors include the work of *Arecchi et al.* [9] on noise-induced hopping between two periodic states, and by *Kautz* [8] on noise-induced or inhibited hopping between a periodic state and a metastable chaotic state. In this Letter, we report a new mechanism for stochastic resonancelike oscillatory motions in the Lorenz equations induced by noise. The stochastic resonancelike behavior is embodied in a Hopf bifurcationlike sequence evicted by noise, where the strength of noise plays the role of a bifurcation parameter. The induced oscillatory motions have very well defined period and amplitude, with the amplitude steadily increasing with the level of noise, until suddenly the motion appears chaotic. When the noise level is not too strong, the noise-induced motions enable objective computation of the largest positive Lyapunov exponent, and thereby qualify as true chaotic motions.

We study the following noise-driven Lorenz equations:

$$\begin{aligned} dx/dt &= -\sigma(x - y) + D\eta_1(t), \\ dy/dt &= rx - y - xz + D\eta_2(t), \\ dz/dt &= xy - bz + D\eta_3(t). \end{aligned} \quad (1)$$

Here  $\langle \eta_i(t) \rangle = 0$ ,  $\langle \eta_i(t)\eta_j(t') \rangle = \delta_{ij}\delta(t - t')$ ,  $i, j = 1, 2, 3$ , where angle brackets denote expectations,  $\sigma = 10$ , and  $b = 8/3$ . Note that  $D^2$  is the variance of the Gaussian noise terms, and thus can be considered to describe the noise strength, and  $D = 0$  describes the clean Lorenz system. When the noise is absent, for  $r \in (24.06, 24.74)$ , the clean system has two stable fixed points,  $C_+ = [\sqrt{b(r-1)}, \sqrt{b(r-1)}, r-1]$  and  $C_- = [-\sqrt{b(r-1)}, -\sqrt{b(r-1)}, r-1]$ , and a strange attractor. Depending on initial conditions, the solution may settle down on any of these three attractors. This is the parameter interval that we shall primarily focus on. For  $r \in (13.926, 24.06)$ , the system exhibits metastable chaotic behavior; i.e., for certain initial conditions, it exhibits “chaoslike” behavior for a very long period before settling down on either  $C_+$  or  $C_-$ .

We assume initially there is no motion; i.e., the system stays at either  $C_+$  or  $C_-$ . When there is no noise, the system will, of course, just stay there. When a very small amount of noise is added, intuitively we would expect the solution to stay close to either  $C_+$  or  $C_-$  and fluctuate. When the parameter  $r$  is away from  $r = 24.74$ , such as  $r = 24.10$ , this is indeed the case, as is shown by Fig. 1(a), where we notice that even though the period of the induced oscillatory motion is well defined [see Fig. 4(c) below], the amplitude varies wildly. However, when  $r$  is close to 24.74, such as 24.72, the oscillatory motion not only has well defined period, but also has very well

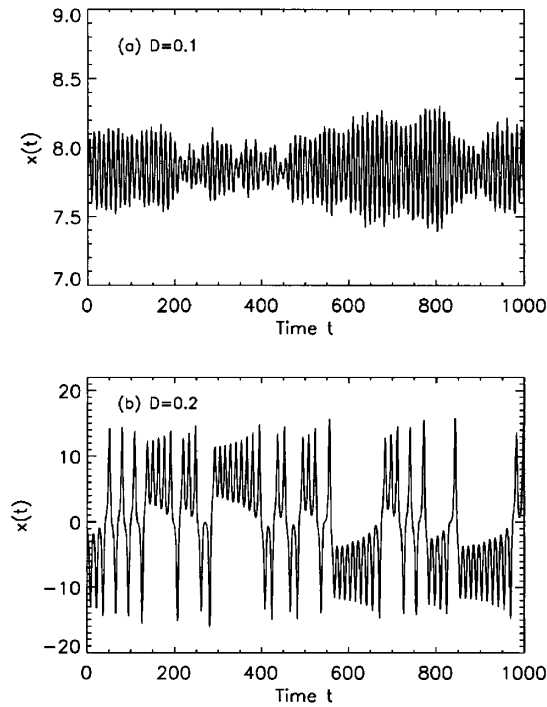


FIG. 1. Time series for the Lorenz equations with  $r = 24.10$ ,  $D = 0.1$  (a) and  $D = 0.2$  (b). The sampling time is  $\delta t = 0.06$ .

defined amplitude, as shown in Figs. 2(a) and 2(b). Also note that the amplitude depends on the noise level. This behavior thus reminds us of the well-known Hopf bifurcation. Here, however, the noise level plays the role of a bifurcation parameter.

To make the above analogy precise, we have examined the variation of the amplitude of the oscillation with the strength of the noise,  $D^2$ , when  $D$  is small. From Fig. 2(d), we indeed observe a square-root dependence of the amplitude on the noise level, characteristic of Hopf bifurcations.

What happens when the noise level is further increased? The amplitude of the oscillatory motions, both the wildly fluctuating case of Fig. 1(a) and the very steady case of Figs. 2(a) and 2(b), keeps increasing with the noise level, until suddenly the motion becomes chaotic, as shown in Figs. 1(b) and 2(c). The noise level which induces this chaotic motions depends on the parameter  $r$ . Examination of the time series of Figs. 1(b) and 2(c) convinces us that the signal is very similar to that generated by the usual chaotic Lorenz attractor.

Let us examine first whether the chaotic signals of Figs. 1(b) and 2(c) can be characterized as true chaotic signals. For this purpose we employ the direct dynamical test for chaos developed in [21], and later used to study noise-induced chaos in [10,11] and the chaotic nature of sea clutter signals [22]. The method involves first embedding the time series,  $\{x(i)\}$ , with the sampling time  $\delta t$ , onto a suitable state space by forming vectors of the form [23]  $X_i = [x(i), x(i + L), \dots, x(i + (m - 1)L)]$ , with  $m$  being the embedding dimension and  $L$  the delay time,

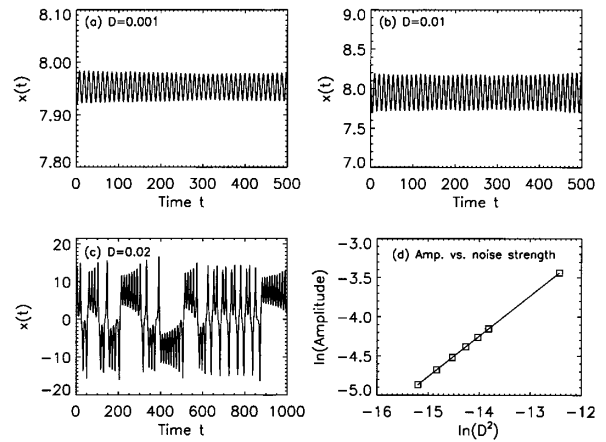


FIG. 2. (a)–(c) Time series for the Lorenz equations with  $r = 24.72$ ,  $D = 0.001$  (a),  $D = 0.01$  (b), and  $D = 0.02$  (c). The sampling time for (a)–(c) is  $\delta t = 0.06$ . In (d), we have plotted, in log-log scale, the variation of the amplitude of the oscillation with the noise strength ( $D^2$ ) for  $D$  not too large. The slope of the linear line is 0.51.

then computing a series of the  $\Lambda(k)$  curves defined by

$$\Lambda(k) = \left\langle \ln \left( \frac{\|X_{i+k} - X_{j+k}\|}{\|X_i - X_j\|} \right) \right\rangle \quad (2)$$

with  $d \leq \|X_i - X_j\| \leq d + \Delta d$ , where  $d$  and  $\Delta d$  are prescribed small distances. The angle brackets denote ensemble averages of all possible pairs of  $(X_i, X_j)$ . The integer  $k$ , called the evolution time, corresponds to time  $k\delta t$ . A pair of  $d$  and  $\Delta d$  is called a shell. The computation is typically carried out for a sequence of shells. For true low-dimensional chaotic systems, the curves  $\Lambda(k)$  vs  $k$  for different shells form a common envelope, when  $k$  is relatively small. The slope of the envelope estimates the largest positive Lyapunov exponent. For systems dominated by noise, the common envelope is absent. Note most conventional methods for estimating the largest positive Lyapunov exponent amount to estimating the Lyapunov exponent by  $\Lambda(k)/k\delta t$ , when  $\|X_i - X_j\|$  is small. When the common envelope is absent, such an estimate of the Lyapunov exponent then sensitively depends on the shell chosen for computation and thus generates incomparable values for the Lyapunov exponent among different researchers.

The results for the computation of the  $\Lambda(k)$  curves for the signals of Figs. 2(c) and 1(b) are shown in Figs. 3(a) and 3(b), where we observe that the common envelope exists for both cases. Hence, both signals of Figs. 1(b) and 2(c) lead to an objective computation of the largest positive Lyapunov exponent, and can be characterized as true chaotic signals. As is expected, with much stronger noise, the two equilibrium points  $C_+$  and  $C_-$  are also annihilated and the signal is still chaotic. However, the  $\Lambda(k)$  curves eventually cease to form a common envelope, a phenomenon similar to that studied in [24]; hence the

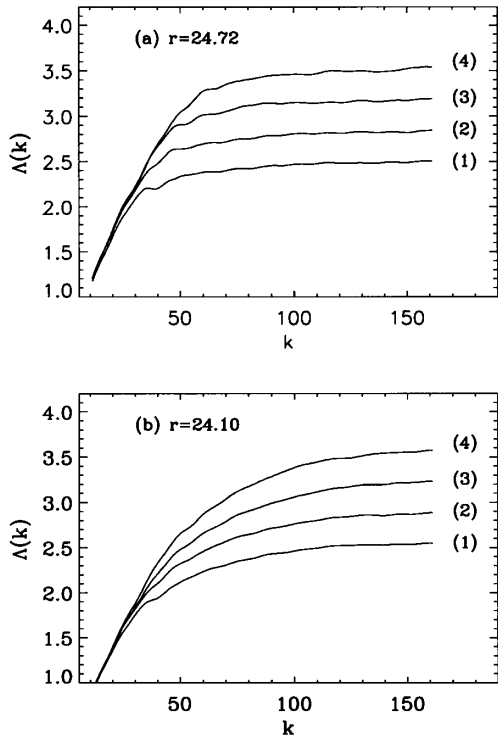


FIG. 3. The  $\Lambda(k)$  curves for the time series of (a) Fig. 2(c) and (b) Fig. 1(b). The numbers 1 to 4 correspond to shells defined by  $[2^{-(i+1)/2}, 2^{-i/2}]$  with  $i = 9$  to 12. The embedding parameters are  $m = 4$  and  $L = 3$ .

chaoslike signals can no longer be characterized as being truly chaotic.

Next let us consider noise-induced oscillatory signals. To better appreciate that these signals have a well defined period and amplitude, we have plotted in Figs. 4(a)–4(c) the power spectral density (PSD) for signals of Figs. 2(a), 2(b), and 1(a). To more clearly show the dependence of the PSD on the noise level, we have normalized PSD by the variance of noise. This way, the value of the sharpest peak directly corresponds to the signal-to-noise ratio. Since Fig. 4 is in logarithmic scale, the normalization does not affect the height of the sharpest peak relative to the background spectrum due to noise. We observe that in all these three signals, the period is very well defined by the (reciprocal of the) sharpest peak in the spectra. The normalized PSD for signals of Figs. 2(a) and 2(b) is several orders of magnitude larger than that for the signal of Fig. 1(a). This clearly says that signals of Figs. 2(a) and 2(b) have much better defined amplitude than that of Fig. 1(a).

For  $r = 24.72$ , we have examined the variation of the normalized PSD corresponding to the sharpest peak vs the noise level. This variation has several maxima; hence the induced oscillatory motions are not simply due to resonancelike behavior. The underlying reason for this behavior is probably that the vector field in the Lorenz equations is very complicated, noting that there are two stable equilibrium points  $C_+$  and  $C_-$ , two unstable limit

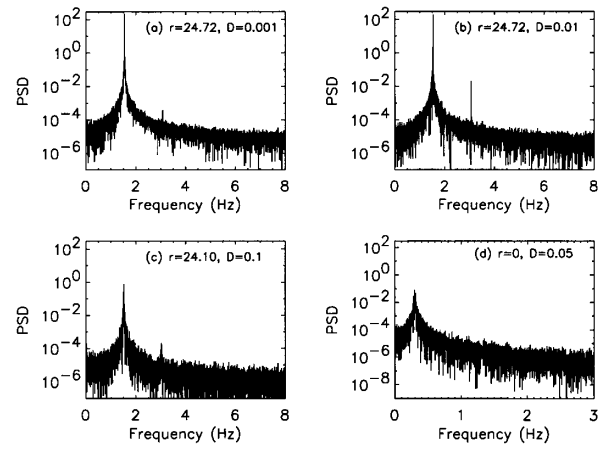


FIG. 4. The power spectral density (PSD) for the time series of (a) Fig. 1, (b) Fig. 1(b), (c) Fig. 2(a), and (d) Fig. 5. It is in logarithmic scale and normalized by the variance of the noise, to ensure that the value of the PSD corresponding to the sharpest peak in the spectrum gives the signal-to-noise ratio.

cycles (with vanishing amplitude near  $r = 24.74$ ), and the strange attractor. The most interesting point here is that when the noise is absent, the Lorenz equations do not allow periodic motions. While conventional stochastic resonance requires a weak periodic forcing, here the oscillatory motions are simply induced by noise.

It has been shown [25] that noise may make the Hopf bifurcation occur slightly before the bifurcation point. To compare between the noise-induced oscillatory motions associated with a Hopf bifurcation and in the Lorenz equations, below we consider the normal form for the Hopf bifurcation with noise:

$$\begin{aligned} du/dt &= -v + u(r - u^2 - v^2) + D_1 \eta_1(t), \\ dv/dt &= u + v(r - u^2 - v^2) + D_2 \eta_2(t), \end{aligned} \quad (3)$$

where  $\eta_i(t)$ ,  $i = 1, 2$ , are independent white Gaussian noise terms with mean 0 and variance 1. Typically,  $D_1$  is taken to be 0, so that the two equations, when written as a second-order differential equation, describe the motion of an oscillator with the  $D_2 \eta_2(t)$  term acting as the stochastic forcing. We have performed two sets of computations,  $D_1 = D_2$  and  $D_1 = 0, D_2 \neq 0$ . Both cases generate similar results. Below we choose  $D_1 = 0$  to present our results. We shall simply write  $D_2 = D$ .

When  $r = 0$ , Hopf bifurcation occurs for the clean system. Figure 5 shows a time series of  $u(t)$  when  $r = 0$  and  $D = 0.05$ . Note that this time series is typical for a small interval of the parameter  $r$  including  $r = 0$ . We observe oscillatory motions with well defined period but wildly varying amplitude, similar to that shown in Fig. 1(a). Figure 4(d) shows the normalized PSD for the signal of Fig. 5. We observe that the normalized PSD for this case is even lower than that for Fig. 1(a). Thus we conclude that the noise-induced oscillatory motions in the Lorenz equations when  $r$  is close to 24.74 are much better

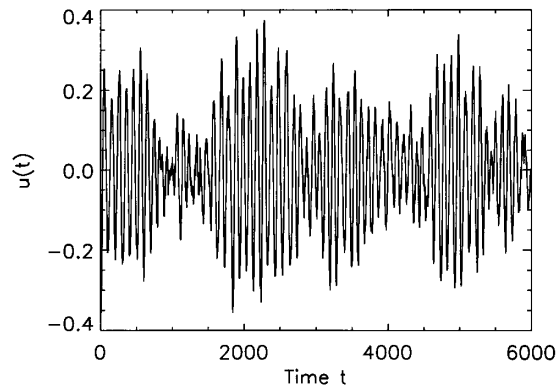


FIG. 5. The time series for the Hopf bifurcation. The sampling time is  $1/30$ .

defined than those associated with the actual Hopf bifurcation. Note that in a typical stochastic resonance, the PSD would show sharp peaks superimposed on a broadband spectra due to noise. However, the background noise spectra of Figs. 4(a) and 4(b) are rather insignificant. Hence, we conclude that the induced oscillatory motions in the Lorenz equations when  $r$  is close to 24.74 are stronger than those due to stochastic resonance.

To briefly summarize, we have observed a Hopf-bifurcation-type sequence and transition to chaos evicted by noise in the Lorenz equations when the parameter  $r$  is close to 24.74. The oscillatory motions induced by noise are better defined than those associated with an actual Hopf bifurcation [described by the normal form of Eq. (3)], as well as stronger than those due to stochastic resonance. When the noise level is not too high, the noise-induced chaoslike motions allow an objective computation of the largest positive Lyapunov exponent, and thus can be characterized as true chaotic signals. Note that when the noise level is above a certain threshold value, neither the equilibrium points  $C_+$  or  $C_-$  nor the noise-induced oscillatory motions can be observed. This behavior may be termed annihilation of some of the coexisting attractors due to noise [26].

In the parameter region we studied, the clean Lorenz equations do not exhibit periodic solutions. Hence, the observed noise-induced oscillatory motions make us surmise that it may be possible for noise to induce a toruslike route to chaos in systems with a single fundamental frequency. This, of course, remains to be seen.

This research is partially sponsored by the Engineering Research Program and the High Performance Networking Program of the Office of Science, U.S. Department of Energy, under Contract No. DE-AC05-00OR22725 with UT-Battelle, LLC.

[1] R. Benzi, A. Sutera, and A. Vulpiani, *J. Phys. A* **14**, L453 (1981).

- [2] L. Gammaitoni, P. Hanggi, P. Jung, and F. Marchesoni, *Rev. Mod. Phys.* **70**, 223 (1998).
- [3] A. R. Bulsara, E. W. Jacobs, and W. C. Schieve, *Phys. Rev. A* **42**, 4614 (1990).
- [4] Z. Y. Chen, *Phys. Rev. A* **42**, 5837 (1990).
- [5] K. Matsumoto and I. Tsuda, *J. Stat. Phys.* **31**, 87 (1983).
- [6] J. P. Crutchfield and B. A. Huberman, *Phys. Lett. A* **74A**, 407 (1980).
- [7] J. P. Crutchfield, J. D. Farmer, and B. A. Huberman, *Phys. Rep.* **92**, 46 (1982).
- [8] R. L. Kautz, *J. Appl. Phys.* **58**, 424 (1985).
- [9] F. Arecchi, R. Badii, and A. Politi, *Phys. Rev. A* **32**, 402 (1985).
- [10] J. B. Gao, S. K. Hwang, and J. M. Liu, *Phys. Rev. Lett.* **82**, 1132 (1999); J. B. Gao, C. C. Chen, S. K. Hwang, and J. M. Liu, *Int. J. Mod. Phys. B* **13**, 3283 (1999).
- [11] K. Hwang, J. B. Gao, and J. M. Liu, *Phys. Rev. E* **61**, 5162 (2000).
- [12] J. Maurer and A. Libchaber, *J. Phys. (Paris), Lett.* **41**, 515 (1980).
- [13] E. Brun, B. Derighette, D. Meier, R. Holzner, and M. Raveni, *J. Opt. Soc. Am. B* **2**, 156 (1985); J. R. Tredicce, F. T. Arecchi, G. P. Puccioni, A. Poggi, and W. Gadomski, *Phys. Rev. A* **34**, 2073 (1986); D. Dangoisse, P. Glorieux, and D. Hennequin, *ibid.* **36**, 4775 (1987); H. G. Solari, E. Eschenazi, R. Gilmore, and J. R. Tredicce, *Opt. Commun.* **64**, 49 (1987); B. K. Goswami, *Phys. Lett. A* **245**, 97 (1998).
- [14] T. Kapitaniak, J. Brindley, and L. Kocarev, *Geophys. Res. Lett.* **22**, 1257 (1995).
- [15] J. M. T. Thompson and H. B. Stewart, *Nonlinear Dynamics and Chaos* (Wiley, Chichester, 1986).
- [16] A. Goldbeter and J.-L. Martiel, *FEBS Lett.* **191**, 149 (1985); D. R. Chialvo and A. V. Apkarian, *J. Stat. Phys.* **70**, 373 (1990).
- [17] J. Foss, A. Longtin, B. Mensour, and J. Milton, *Phys. Rev. Lett.* **76**, 708 (1996).
- [18] P. Cordo, J. T. Inglis, S. Verschuere, J. J. Collins, D. M. Merfeld, S. Rosenblum, S. Buckley, and F. Moss, *Nature (London)* **383**, 769 (1996).
- [19] E. Simonotto, M. Riani, C. Seife, M. Roberts, J. Twitty, and F. Moss, *Phys. Rev. Lett.* **78**, 1186 (1997).
- [20] I. Merk and J. Schnakenberg, *Biol. Cybern.* **86**, 111 (2002).
- [21] J. B. Gao and Z. M. Zheng, *Europhys. Lett.* **25**, 485 (1994); *Phys. Rev. E* **49**, 3807 (1994).
- [22] S. Haykin and S. Puthusserypady, *Chaos* **7**, 777–802 (1997); J. B. Gao and K. Yao, in *Proceedings of the IEEE Radar Conference 2002, Long Beach, CA* (IEEE, Piscataway, NJ, 2002), p. 500.
- [23] N. H. Packard, J. P. Crutchfield, J. D. Farmer, and R. S. Shaw, *Phys. Rev. Lett.* **45**, 712 (1980); F. Takens, in *Dynamical Systems and Turbulence*, Lecture Notes in Mathematics Vol. 898, edited by D. A. Rand and L. S. Young (Springer-Verlag, Berlin, 1981), p. 366.
- [24] J. B. Gao, *Physica (Amsterdam)* **106D**, 49 (1997).
- [25] K. H. Hoffman, *Z. Phys. B* **49**, 245 (1982); A. Juel, A. G. Darbyshire, and T. Mullin, *Proc. R. Soc. London Ser. A* **453**, 2627 (1997).
- [26] A. N. Pisarchik and B. K. Goswami, *Phys. Rev. Lett.* **84**, 1423 (2000).